Published in final edited form as:
Traffic. 2011 July ; 12(7): 902–911. doi:10.1111/j.1600-0854.2011.01194.x.

A Role for Rab7 in the Movement of Secretory Granules in Cytotoxic T Lymphocytes

Tiziana Daniele[1,2,†], **Yvonne Hackmann**[1], **Alex T. Ritter**[1], **Matt Wenham**[1,†], **Sarah Booth**[3,†], **Giovanna Bossi**[†,**], **Michael Schintler**[4,5], **Michaela Auer-Grumbach**[4,5], and **Gillian M. Griffiths**[1,*,†]

[1]Cambridge Institute for Medical Research, Hills Road, Cambridge CB2 0XY, UK

[2]San Raffaele Scientific Institute (DIBIT), via Olgettina 58, 20132 Milano, Italy

[3]The Weatherall Institute of Molecular Medicine, Headington, Oxford OX3 9DS, UK

[4]Institute of Human Genetics, Medical University of Graz, Harrachgasse 21, 8010 Graz, Austria

[5]University Clinic of Internal Medicine, Division of Endocrinology and Nuclear Medicine, Medical University of Graz, Harrachgasse 21, 8010 Graz, Austria

Abstract

Cytotoxic T lymphocytes (CTL) are potent killers of virally infected and tumorigenic cells. Upon recognition of target cells, CTL undergo polarized secretion of secretory lysosomes at the immunological synapse (IS) that forms between CTL and target. However, the molecular machinery involved in the polarization of secretory lysosomes is still largely uncharacterized. In this paper, we investigated the role of Rab7 in the polarization of secretory lysosomes. We show that silencing of Rab7 by RNA interference reduces the ability of CTL to kill targets. GTP-bound Rab7 and Rab interacting lysosomal protein, RILP, interact and both localize to secretory lysosomes in CTL. Over-expression of RILP recruits dynein to the membranes of secretory lysosomes and triggers their movement toward the centrosome. Together, these results suggest that Rab7 may play a role in secretory lysosome movement toward the centrosome by interacting with RILP to recruit the minus-end motor, dynein.

Keywords

Bicaudal; CTL; CMT2B; dynein; lymphocytes; lysosomes; ORP1L; polarization; Rab7; RILP; secretion

Cytotoxic T lymphocytes (CTL) play an essential role in immunity, as they are responsible for the recognition and clearance of both virally infected and tumorigenic cells. Upon recognition of target cells, CTL undergo a drastic reorganization of actin and microtubules that leads to the polarization of the centrosome toward the immunological synapse (IS)

*Corresponding author: Gillian M. Griffiths, gg305@cam.ac.uk.
**Present address: Immunocore, 57c Milton Park, Abingdon, OX14 4RX, UK
†This work was started at the Sir William Dunn School of Pathology, South Parks Road, Oxford OX1 3RE, UK.

Europe PMC Funders Author Manuscripts

formed with the target. Secretory lysosomes, also known as lytic granules, containing the lytic protein perforin, use minus-end-directed movement along microtubules to reach the IS where they release their contents and destroy the target (1). Precisely how this minus-end movement is controlled in CTL is not known.

In non-immune cells, small GTPases have been shown to be indispensable for regulated organelle movement. The function of small GTPases is regulated by their nucleotide binding state with GTP being the activator that mediates relocalization of small GTPases to membranes. In particular, Rab7 has been shown to localize to late endosomes/lysosomes (2) and to control the minus-end-directed movement of these organelles along microtubules in non-immune cells (3–5). Rab7 can recruit dynein via the effector proteins oxysterol-binding related protein (ORP)1L and Rab interacting lysosomal protein (RILP) (7), with over-expression of these proteins leading to clustering of lysosomes in HeLa and melanoma cell lines (8,9). Conversely, over-expression of a RILP mutant, lacking the dynein-binding domain, causes the dispersion of lysosomes (8).

Other mechanisms for dynein recruitment and regulation of organelle distribution also exist. Bicaudal-D proteins bind dynein directly via the N-terminus, and over-expression of Bicaudal-D2 N-terminus disrupts the dynein-based distribution of organelles (10).

In CTL, dynein is recruited to the IS and plays a role in the polarization of the centrosome during synapse formation (11,12). However, little is known about if and how dynein is recruited to the secretory lysosomes or its function in the polarization of secretory lysosomes. In this paper, we sought to investigate the role of Rab7 in CTL. We find that Rab7 and RILP both localize to secretory lysosomes in CTL. GTP-bound Rab7 interacts with RILP, which recruits dynein to secretory lysosomes, allowing minus-end-directed movement toward the centrosome.

Europe PMC Funders Author Manuscripts

Results

Rab7, but not the Bicaudal proteins BICD1 and BICD2, localizes to secretory lysosomes

We asked whether cytotoxic lymphocytes (CTL) express Rab7, RILP, BICD1 and BICD2. Cell lysates from human CTL (hCTL) were separated by SDS–PAGE and probed with antibodies against Rab7, BICD1 and BICD2. By western blotting (WB) we detected a single band at <21 kDa corresponding to Rab7 and doublets at <100 kDa corresponding to either BICD1 or BICD2 (Figure 1A). We examined endogenous RILP expression in CTL at both the RNA and protein levels. Using PCR we amplified a 216-bp fragment corresponding to the region coding for the dynein-binding domain of RILP (Figure 1B). This amplification gave a strong band in cDNA from HeLa cells, and a weaker band in cDNA from hCTL. The identity of the PCR product was confirmed by sequencing and expression of RILP protein was assessed using an anti-RILP antiserum. The specificity of the antiserum was confirmed using cell lysates from the rat basophilic leukkemia (RBL) mast cell line, transfected with either GFP-Rab7 (lane 1) or GFP-RILP (lane 3). A 45-kDa band corresponding to endogenous RILP was visible in both RBL lanes, and in addition an approximately 70-kDa band corresponding to GFP-RILP was present in lane 3, but not lane 1. A 45-kDa band was also present in the hCTL lysate supporting the idea that RILP protein is expressed in CTL

albeit at a low level (lane 2). The same filters were reprobed for Rab7. A 50-kDa band corresponding to GFP-Rab7 was only observed in GFP-Rab7 transfected RBL (lane 1), while a band of 25 kDa corresponding to endogenous Rab7 was detected in both RBL and CTL (Figure 1C, lanes 1–3).

Using a polyclonal anti-Rab7 serum that recognizes only membrane-associated Rab7, we were able to colocalize Rab7 with Lamp1 in up to 5% of CTL, demonstrating that Rab7 is able to localize to secretory lysosomes (Figure 2A). In contrast, BICD1 colocalized with the centrosomal marker, acetylated tubulin, distinct from lysosomal and Golgi markers, and BICD2 also clustered close to the centrosome, with no apparent overlap with GM130 in these cells (Figure 2B).

Rab7 localizes to secretory lysosomes in CTL

To test whether Rab7 regulates the distribution of lysosomes in hCTL, we over-expressed the dominant negative (inactive, GDP-bound, T22N) and the dominant positive (active, GTP-bound, Q67L) mutants. Mouse CTL (mCTL) were transiently transfected with constructs coding for the GFP-tagged version of wild-type (wt) and mutant Rab7 and imaged either live (Figure 2C) or fixed (Figure 2D). Both live and fixed mCTL showed that wt and active forms of GFP-Rab7 associated with secretory lysosomes as imaged with lysotracker (live) or Lamp1 (fixed). By contrast, the inactive mutant of Rab7 was cytosolic and showed greatly reduced colocalization with both Lysotracker and Lamp1, while the active form of Rab7 appeared more tightly associated with the secretory lysosomes, with less cytosolic staining. All transfectants for each construct showed the same localization pattern.

Knock-down of Rab7 impairs killing in human and murine CTL

To address the role of Rab7 in the function of CTL, we knocked down the protein by transfection with small interfering RNA oligonucleotides (siRNAs). To silence the expression of endogenous Rab7, we transfected both murine and hCTL with either 3 μg of a Smart pool of four siRNAs or 3 μg of oligonucleotide #4 (see *Materials and Methods*). The knock-down of Rab7 was verified by WB (using the antibody developed in this study, and all siRNAs gave a reduction in Rab7 protein levels of >75%, with RNA Rab7 #4 providing a reduction of >90%) and sample loading assessed by probing for actin (Figure 3A,B). When we evaluated the killing ability of murine or hCTL treated with a non-targeting RNA (NT RNA) or with a Rab7-specific siRNA (RNA Rab7 #4), we found a reduction in killing of >25% with the Rab7-specific siRNA (Figure 3C,D) as compared to controls.

V162M mutation in Rab7 neither enhances nor impairs CTL killing

As impaired Rab7 function decreased CTL killing, we asked whether dominant positive mutations in Rab7 affected CTL killing. Patients affected by the Charcot Marie Tooth syndrome type 2 B (CMT2B) show unregulated guanine nucleotide exchange and exhibit impaired GTPase activity. Therefore, Rab7 is more abundant in its GTP-, membrane-bound form, which results in an increased interaction with some of the downstream effectors (13–15).

Europe PMC Funders Author Manuscripts

We stained hCTL lines derived from a healthy donor and from a previously described CMT2B patient with the V162M mutation (16), with antibodies against Rab7, Lamp2 and dynein (Figure 4A). Rab7 overlaps with Lamp2 structures, consistent with recruitment of the active form of Rab7 to secretory lysosomes in both hCTL and CMT2B cells. Staining for Lamp2 and γ-tubulin (markers of lysosomes and the centrosome, respectively) suggested that there might be an increased clustering of lysosomes around the centrosome in CMT2B cells (average distance = 5.16 ± 0.97 μm) as compared to the distribution in CTL from a healthy donor (average distance = 7.11 ± 1.50 μm, $p < 0.001$ with Student's t-test). The overall levels of Lamp2 were equivalent between hCTL from healthy donors and CMT2B patients (Figure 4C). The altered distribution may therefore suggest that the V162M variant of Rab7 expressed in these cells might increase lysosomal movement toward the centrosome. When CTL-target conjugates were formed, labeling with antibodies against cathepsin D and tubulin showed that both the centrosome and lysosomes polarized to the IS in CMT2B and healthy donor cells (Figure 4B), and patient cells showed a killing capacity comparable to CTL derived from a healthy donor (Figure 4D).

Rab7 interacts with RILP in CTL

RILP has been shown to recruit dynein to late endosomes (6). To test the possible recruitment of RILP to lysosomes by Rab7, hCTL lysates were treated with GTPγS in order to lock Rab7 in its active GTP-bound state, and either recombinant GST (glutathione S-transferase)-RILP or GST alone was used to pull down Rab7 from hCTL lysates. Pull down of Rab7 was detected by WB (Figure 5A). GST-RILP pulled down Rab7 from hCTL, while GST alone did not, demonstrating that Rab7 and RILP can interact in CTL. This result is supported by the observation that endogenous Rab7 colocalizes with RILP in hCTL over-expressing GFP-RILP (Figure 5B). Over-expression of GFP-RILP causes secretory lysosomes to cluster and the colocalization of antibody-labeled endogenous Rab7 with GFP-RILP is very clear. These data support a model in which Rab7 might recruit RILP to secretory lysosomes.

We asked whether GFP-RILP over-expression might compensate for Rab7 depletion, or whether Rab7 was necessary for effective killing, by using siRNA to knock down Rab7 expression in hCTL expressing GFP-wt RILP.

Rab7 was depleted only when treated with the Rab7-specific siRNA (Figure 5C). Rab7-depleted CTL over-expressing GFP-RILP showed the same 30% reduction in killing relative to controls (Figure 5D) in which GFP-RILP was not over-expressed (Figure 3D). This indicates that Rab7 is required for optimal killing and that over-expression of RILP cannot overcome this defect.

RILP recruits dynein to secretory lysosomes in CTL

In CTL over-expressing GFP-RILP, Rab7-labelled lysosomes appeared tightly clustered next to the nucleus (Figure 5B). We confirmed that RILP localized to secretory lysosomes in both mouse and hCTL, by labeling with antibodies to either the soluble secretory lysosome protein, perforin for hCTL, or Lamp2 for mCTL. In untransfected CTL, secretory lysosomes were distributed throughout the cell (Figure 6A). In CTL transfected with GFP-RILP,

secretory lysosomes were tightly clustered with perforin and Lamp2 colocalized with GFP-RILP in hCTL and mCTL, respectively, confirming the secretory lysosome localization of RILP.

We asked whether, once RILP is recruited to the membranes of secretory lysosomes, it might then recruit dynein. We examined the localization of dynein in CTL over-expressing GFP-wt RILP or GFP-ΔN RILP, which lacks the dynein-binding domain (17) (Figure 6B). In untransfected CTL, dynein gave a diffuse cytoplasmic and centrosomal distribution (Figure 6B). GFP-wt RILP localized to secretory lysosomes and triggered clustering around the centrosome (1). In CTL transfected with GFP-wt RILP, dynein was recruited to secretory lysosomes, colocalizing with GFP-wt RILP in both mouse and hCTL (Figure 5B). In contrast, CTL transfected with GFP-ΔN RILP showed neither secretory lysosomes clustering nor recruitment of dynein to lysosomal membranes. Similarly, CTL expressing GFP-ORP1L, which has been shown to form a tripartite complex with Rab7 and RILP in HeLa cells (7), did not show recruitment of dynein or lysosomal clustering in CTL (Figure 6B).

These data support a model in which active Rab7 interacts with RILP, which is able to recruit dynein to the secretory lysosomes of CTL, causing minus-end-directed movement of these organelles toward the centrosome.

Discussion

CTL destroy their targets by release of the contents of secretory lysosomes (lytic granules), which are delivered to the IS by minus-end-directed movement along microtubules. The precise site of delivery is determined by the point where the centrosome docks within the synapse (13). Once the centrosome is docked, the lytic granules migrate along the microtubules in a minus direction to deliver their contents at the IS. Previous studies have shown that over-expression of RILP triggers clustering of lytic granules at the centrosome (13). In this paper, we have examined the role of Rab7 and RILP in lytic granule movement toward the IS.

We examined the expression and localization of Rab7, RILP, ORP1L, BICD1, BICD2 and dynein in CTL. Staining for endogenous proteins, we found that dynein, BICD1 and BICD2 are all localized to the centrosome, while the membrane-bound form of Rab7 can localize to secretory lysosomes, colocalizing with Lamp1. Studies on RILP have been hampered by the lack of available antibodies that recognize the endogenous protein, and the majority of studies rely on over-expression of RILP-GFP. Although we were able to detect low levels of endogenous RILP protein expression in hCTL by WB, none of the antibodies currently available detects endogenous RILP by immunofluorescence. Using over-expression we were able to show that GFP-RILP localizes to the lytic granules and is able to recruit dynein to secretory lysosomes. GFP-ORP1L also localizes to the lytic granules but, unlike RILP, its over-expression does not increase the recruitment of dynein to the granule membranes in CTL. These results suggest that one role of Rab7 on secretory lysosomes of CTL might be to recruit RILP and dynein to the lytic granules, and facilitate minus-end-directed movement along microtubules.

We used siRNA to deplete Rab7 in CTL. Both pooled and single siRNAs were tested and it was possible to knock down the level of Rab7 protein in both murine and hCTL by more than 90% as assessed by WB (Figures 3A,B). We confirmed the ability of GTP-bound Rab7 in CTL to interact with RILP biochemically using a pull-down assay and were able to show that both localize on the lytic granules (Figure 5).

Use of siRNA to knock-down Rab7 allowed us to carry out functional assays. Rab7-depleted CTL showed a consistent reduction in their ability to kill target cells to 60–70% of the levels of mock/control RNA-treated cells. A number of reasons might explain why there is not a more complete loss of killing. First, although knock-down of Rab7 was good it was still possible to detect a faint band by WB, demonstrating that low levels of Rab7 remained. CTL are very efficient killers and it is possible that only low levels of Rab7 are required. Second, Rab7 has other roles in cells (19), and it is possible that Rab7 is not the only effector protein that recruits dynein in CTL. Rab34 is also known to modulate dynein function via RILP (20), although we were not able to detect Rab34 in CTL (data not shown). We cannot rule out that BICD1 and BICD2 might also be recruited to the lytic granules by other effectors, such as Rab6 (21). However, as Rab6 is usually associated with the Golgi complex and we do not see a clear association of either BICD1 and BICD2 with Golgi markers in CTL, this does not seem likely. Another possibility is that other minus-end motors, such as those of the KIF14 family [unconventional kinesins comprising a C-terminal motor domain (22)], could be involved. It might even be possible that plus-end-directed motor proteins play a role, because the net transport along microtubules could result from the balance between the activity of motor proteins with opposing directions (reviewed in 21).

The dominant active form of Rab7 with the V162M mutation found in some patients with Charcot Marie Tooth 2B syndrome supported the idea that active Rab7 does not impair CTL function. CMT2B is characterized by sensory neuropathy and frequent infections in the foot (18,24). The mechanism by which Rab7 mutations induce the development of peripheral neuropathy is only beginning to be investigated (16,23,24). Rab7 has been shown to regulate the retrograde transport of a vesicular compartment implicated in neurotrophin traffic (27,28). All the Rab7 mutations identified in Charcot Marie Tooth 2B patients behave as dominant positive mutants of Rab7 both in terms of the relative abundance of the GTP-bound form and of their increased binding to some of their downstream effectors (2,5,14–16). Our images suggest that the dominant active Rab7 (V162M) expressed in CMT2B CTL might cause the lytic granules in these cells to be more tightly clustered around the centrosome than those in CTL from healthy donors, although increased dynein recruitment could not be seen. As granules need to cluster around the centrosome to reach the IS (13), then killing is not impaired by increasing clustering.

Our results support the idea that Rab7 is likely to play a role in transporting secretory lysosomes to the IS in CTL. Our results are consistent with a model in which Rab7 on secretory lysosomes interacts with RILP, which recruits dynein, enabling minus-end-directed movement of these organelles toward the IS, a critical step in the function of CTL.

Materials and Methods

Reagents and antibodies

Primary polyclonal antibodies—Rabbit anti-cathepsin D (Upstate Biotechnology), anti-tubulin (Sigma), anti-Rab7 (Sigma) were developed in this study; anti-Rab7 recognizing membrane bound Rab7 by immunofluorescence was a gift from Dr A. Wandinger-Ness (The University of New Mexico Health Sciences Center, New Mexico, USA); anti-RILP (Abcam), anti-RILP from Jacques Camonis (Institut Curie, Paris) and anti-BICD1 and anti-BICD2 from Dr A. Akhmanova (Erasmus Medical Center, Rotterdam, The Netherlands).

Primary monoclonal antibodies—Anti-CD3 (OKT3) (Cambridge Bioscience), anti-CD3 (UCHT1) (Pharmigen), mouse-anti-Lamp1 (H4A3), rat anti-murine (1DB4), mouse anti-human (H4B4) and rat anti-murine (ABL93) Lamp2, mouse-anti-human-CD63 (H5B6) were all from Developmental Studies Hybridoma Bank (Iowa). Mouse-anti-perforin (G9) (Pharmigen),-acetylated tubulin, and -actin were from Sigma and mouse anti-dynein intermediate chain (human and murine) (Chemicon International). Mouse anti-tubulin (TAT-1) was a gift from K. Gull (Oxford University, UK). Lysotracker, Alexa 488, Alexa 543, Alexa 405 and Alexa 633 secondary antibodies were obtained from Molecular Probes (Invitrogen). All chemical reagents were of analytical grade or higher and purchased from Sigma, unless otherwise specified.

RNA extraction, cDNA preparation and RT-PCR

RNA was isolated from cell pellets using the PureLink™ Micro-to-Midi total RNA purification System (Invitrogen). cDNA was generated using the Superscript II RT-PCR kit (Invitrogen).

To study the expression of RILP in hCTL, a 216-bp fragment was amplified from cDNA using the following primers: forward: 5′-**CCTACTTCCAGCGGGAGC**-3′ and reverse: 5′-**TCTGTATTTTGGACTCCGGG**-3′.

For PCR amplification, BIOTAQ DNA Polymerase (Bioline) was used with 2 mM $MgCl_2$ and under the following cycling conditions: 95°C for 10 min followed by 40 cycles of 95°C for 30 seconds, 55°C for 30 seconds and 72°C for 30 seconds. The reaction was completed by an elongation at 72°C for 10 min, and analyzed on a 2% agarose gel.

DNA constructs

cDNA encoding human HA-tagged Rab7 was obtained from UMR cDNA Resource Center and subcloned into pEGFP-C, or pMaxFP–Green-C or pMaxFP–Red-C vectors (Clontech and Amaxa, respectively) as a *Hin*dIII/*Xho*I fragment.

The dominant negative and positive mutants of human Rab7 were generated by site-directed mutagenesis (Stratagene) using the following primers, respectively: T22N: forward 5′-**GGAGATTCTGGAGTCGGGAAG<u>AAC</u>TCACTCATGAACCAGTATG**-3′ and reverse: 5′-**CTTATTCACATACTGGTTCATGAGTGA<u>GTT</u>CTTCCCGACTCCAGAAT**-3′; Q67L: forward 5′-**TGGGACACAGCAGGA<u>CTG</u>GAACGGTTCCAGTCT**-3′ and

reverse 5′-**AGACTGGAACCGTTCCAGTCCTGCTGTGTCCCA**-3′. The ORP1L and RILP constructs were a kind gift of Dr Jacques Neefjes (The Netherlands Cancer Institute, Amsterdam, The Netherlands). RILP was encoded by the full-length cDNA sequence (NM031430.2). The N-RILP mutant was generated by PCR using the following primers: forward 5′-**CGCAGATCTGGGCGGCCCGGGCACC**-3′ and reverse 5′-**CGCAAGCTTTCAGGCCTCTGGGCGGC**-3′.

For PCR amplification, the Expand High Fidelity^{PLUS} PCR system (Roche) was used under the following cycling conditions: 95°C for 2 min followed by 50 cycles, each consisting of 95°C for 45 seconds, 58°C for 45 seconds, and 72°C for 1 min. The reaction was completed by an elongation at 72°C for 10 min, and analyzed on a 1% agarose gel. The PCR product was subcloned into pEGFP-C or pMaxFP–Green-C or pMaxFP–Red-C vectors as a *Bgl*II/*Hin*dIII fragment.

GFP-RILP was subcloned into the pHR'SINcPPT-SEW vector as previously described (12).

All constructs were confirmed by ABI sequencing before use.

Anti-Rab7 antibody preparation

A construct encoding recombinant glutathione S-transferase-tagged human full-length Rab7 was generated by amplification of the *Rab7* gene by PCR using the Expand^{PLUS} polymerase (Roche) and the following primers: forward 5′-**CGCGAATTCACCTCTAGGAAGAAAGTGTTGC**-3′ and reverse 5′-**CGCCTCGAGTCAGCAACTGCAGCTTTCTGC**-3′ and subcloning into the pGEX4T1 vector as a *Eco*RI/*Sac*I fragment. The construct was confirmed by ABI sequencing and used to transform chemically competent DH5 *Escherichia coli* strain. The GST-tagged Rab7 protein was purified as described previously (29) and sent to Cambridge Research Biochemicals for immunization. The serum obtained from rabbits was tested in human cells transfected with the recombinant wt, dp and dn GFP-tagged version of Rab7 both in immunofluorescence studies and by WB.

Cell culture

Murine CTL (mCTL) were derived from C57 BL/6 mice. Freshly isolated spleens were homogenized through a 70-μm strainer (BD) with the plunger from a 2-mL syringe. Splenocytes were then washed once with IMDM (Invitrogen) containing 10% fetal calf serum (FCS) and incubated with an equal number of BALB/c splenocytes irradiated with 3000 Rad in IMDM containing 10% FCS, 100 U/mL recombinant interleukin-2 (rIL-2, Roche), 55 μM mercaptoethanol (Invitrogen) and 2 mM glutamine (Invitrogen). After 5–7 days, mCTL were isolated over Histopaque (Sigma), and cultured for 2–5 days before use for staining, transfection or further rounds of stimulation. OT-1 transgenic CTL were stimulated with OVA peptide as previously described (30).

hCTL were grown in RPMI (Invitrogen) supplemented with 100 U/mL of recombinant IL-2, 5% human serum, 1 mM sodium pyruvate (Invitrogen), 0.075% sodium bicarbonate (Invitrogen), 55 μM mercaptoethanol, and 2 mM glutamine. Cells were stimulated with an equal number of 3000 Rad-irradiated PBMCs. hCTL were used for transfection/transduction

between day 7–8 and day 14–15 after stimulation (active proliferation phase). Cells were cultured till day 28–32 before being restimulated as stated above.

P815 target cells were maintained in RPMI, 10% FCS and Hek293T cells were grown in DMEM, 10% FCS. All cells were grown at 37°C in a humidified incubator with 8% CO_2 (Binder).

Lentiviral production and transduction

The transfer vector plasmids used in this study are: the envelope plasmid pMD.G (29), the packaging plasmid pCMVR8.91 and the self-inactivating transfer plasmid pHR'SINcPPT-SGW (31,32). To generate VSV-G pseudotyped vectors, Hek293T cells were transfected with the three plasmids: pCMVR8.91, pMD.G and pHR'SINcPPT-SGW. Seventy percent confluent Hek293T cells (grown in 75 cm^2 flasks) were transfected with a total of 14 g of plasmid DNA by means of the TransIT®-Express transfection reagent (Mirus Bio) according to the manufacturer's instructions: 4 μg of the envelope plasmid, 4 μg of the packaging plasmid and 6 μg of the transfer vector plasmid. Seventy-two hours after transfection, the medium was harvested, passed through a 0.22-μm filter, and the vector particles were concentrated by ultracentrifugation at 30 000 × ***g*** for 90 min. The pellet was resuspended in 150 μL of growth medium and stored at −80°C. hCTL were transduced with a multiplicity of infection of 1 (1 viral particle/cell), and expression of exogenous GFP-tagged proteins was assessed after 72 h.

Transient transfection and RNA interference

Five million mCTL, after two, three or four rounds of stimulation and 5–7 days after stimulation, were nucleofected with 5 μg of DNA using an Amaxa nucleofector II, programme X-001 and the mouse T cell nucleofection kit, according to the manufacturer's protocol. After 3–6 h, murine T cells were pelleted and resuspended in growth medium.

Five million hCTL, 8–15 days after stimulation with irradiated buffy coat cells, were nucleofected with 5 g of DNA using an Amaxa nucleofector II, programme X-005 and the human T cell nucleofection kit, according to the manufacturer's protocol. Nucleofected human T cells were initially incubated in hTC/LGM-3 medium (Lonza) and, after 3–6 h, pelleted and resuspended in growth medium.

siRNAs were purchased from Dharmacon [Thermofisher; catalogue number M-010388-00-0005 (Smart pool) and MU-010388-00-0005 (set of four Upgrade siRNA duplexes) for human Rab7, M-040859-00-0005 (Smart pool) and MU-040859-00-0005 (set of four Upgrade siRNA duplexes) for murine Rab7, and D-001810-10 for ON-TARGETplus siCONTROL non-targeting pool] and 3 μg nucleofected using an Amaxa nucleofector II (Lonza), as described above.

The four oligonucleotides present in the murine Rab7 pool that were also tested separately were:

#1 (5′-**GUACAAAGCCACAAUAGGAUU**-3′),

#2 (5′-**AAACAACAUUCCUUACUUCUU**-3′),

#3 (5′-**AAACAAGAUUGACCUGGAAUU**-3′),

#4 (5′-**AAGUGGAACUGUACAAUGAUU**-3′).

The four oligonucleotides present in the human Rab7 pool that were also tested separately were:

#1 (5′-**CUAGAUAGCUGGAGAGAUGUU**-3′),

#2 (5′-**GUACAAAGCCACAAUAGGAUU**-3′),

#3 (5′-**AAACGGAGGUGGAGCUGUAUU**-3′),

#4 (5′-**CGAAUUUCCUGAACCUAUCUU**-3′).

All of the experiments reported were performed in mCTL and hCTL using the Smart pool of the four oligonucleotides, and then repeated with at least two different single oligonucleotides (mainly with siRNA #4 as it gives the strongest knock-down, Figure 3).

Cytotoxicity assay

The 2.5×10^6 hCTL or dilutions as shown in the figures were incubated with 10^5 P815 target cells (with 1 μg/mL anti-CD3 for hCTL) for 4 h at 37°C. The assay was performed using the Cytotox 96 kit (Promega), according to the manufacturer's protocol.

Immunofluorescence

CTL were washed twice with serum-free medium, plated in serum-free medium onto glass slides for 15 min before complete media containing sera was added for further 15 min. For conjugate formation, CTL were mixed with an equal number of P815 target cells before plating onto glass multi-well slides (Hendley, Essex).

The cells were fixed with −20°C-cold methanol for 5 min, washed with PBS, and blocked with 1% goat serum in PBS for at least 20 min or, alternatively, with 4% paraformaldehyde (PFA, Electron Microscopy Sciences) in PBS for 10 min at room temperature, washed with PBS and permeabilized for 30 min in 0.1% (w/v) saponin, 0.5% (w/v) BSA and 50 mM NH_4Cl in PBS (blocking buffer). Afterwards, cells were incubated for 2 h with primary antibody, washed three times in PBS, incubated for 1 h with the secondary (Alexa-labelled) antibody, washed three times in PBS, and finally mounted in Mowiol (Calbiochem).

Samples were imaged using a Zeiss LSM 510 confocal laser-scanning microscope. Optical sections were obtained under a 63× or a 100× oil-immersion objective at a definition of 1024 × 1024 pixels (average of four or eight scans), adjusting the pinhole diameter to 1 Airy unit for each emission channel to have all of the intensity values between 1 and 254 (linear range). Images were processed using Zeiss LSM image browser (www.zeiss.com) and Adobe Photoshop. Figures 2B were imaged using the Andor Revolution Spinning Disk microscope and processed using IQ software (Andor).

Quantification of the distance of lysosomes from the centrosome

Measurements were performed on three sets of 10 cells, each from independent experiments. Images of CMT2B patient or healthy donor cells were acquired with the same microscope

settings (i.e. laser power, detector amplification). Optical sections (200 nm thick) of entire cells were acquired by means of the Z-stack function of the LSM510 software (Zeiss), and the background subtracted. Sampling of cells was performed randomly. The identification of 'objects' on the basis of their staining intensity (lysosomes and microtubule organising center (MTOC)) and their spatial 3D coordinates were obtained with the VOLOCITY software from Improvision (Perkin Elmer). The lysosomal distance from the MTOC was determined mathematically, where subscripts L and M indicate lysosomes or the MTOC, respectively.

Western blotting

Cell pellets were washed once with ice-cold PBS, lysed at 1×10^7 cells/mL in lysis buffer containing 2% Nonidet P-40, 150 mM NaCl, 50 mM Tris–HCl pH 8.0, 1 mM $MgCl_2$ and complete protease inhibitor (Boehringer), and incubated for 30 min on ice. Supernatant was centrifuged at 16,000 g for 15 min at 4°C to remove nuclei and membranes. Samples were prepared by adding 2× sample buffer and boiling for 5 min at 95°C before loading onto the gel. Proteins were separated by SDS–PAGE and transferred to nitrocellulose membranes (Hybond, GE Healthcare). Strips containing the proteins of interest were incubated in 1% (w/v) BSA in PBS containing 0.05% (v/v) Tween-20, pH 7.5 (blocking buffer), for 1 h at room temperature and then with fresh blocking buffer containing the primary antibody at its working concentration. After 2 h incubation at room temperature, or overnight at 4°C, the antibodies were removed and the strips washed with PBS containing 0.05% (v/v) Tween-20 for 3 × 10 min. Strips were incubated for 1 h with the appropriate horse radish peroxidase (HRP)-conjugated secondary antibody and washed 3 × 10 min with PBS containing 0.05% (v/v) Tween-20 and once with PBS. Western blots were developed using the chemiluminescent method (ECL, GE Healthcare). The antibody was removed by incubation in stripping buffer (62.5 mM Tris–HCl, pH 6.7, 2% SDS, 100 mM-mercaptoethanol) at 55°C for 30 min. Bands were quantified by densitometric analysis using the NIH IMAGE 1.60 programme. The quantification of each band associated with the Rab7/actin/GFP antibody was normalized for the signal of the corresponding control (mock/non-targeting RNA transfected cells).

Production of GST-RILP wt and in vitro interaction with Rab7

GST-RILP was generated by PCR using the following primers: forward 5′-**cggcgaattcatggagcccaggagggcg**-3′ and reverse 5′-**cggcgcggccgctcaggcctctggggcgg**-3′. RILP was encoded by the full-length cDNA sequence (NM031430.2). For PCR amplification, Pfu DNA polymerase was used under the following cycling conditions: 95°C for 2 min followed by 30 cycles, each consisting of 95°C for 60 seconds, 56°C for 60 seconds, and 72°C for 2 min. The reaction was completed by an elongation at 72°C for 10 min, and analyzed on a 1% agarose gel. The PCR product was subcloned into pGEX-4T1 vector as an *Eco*RI/*Not*I fragment to produce GST fusion protein. This construct was transformed into *E. coli* strain BL21. Transformed bacteria were grown at 37°C in antibiotic-containing medium until optical density (OD) reached 0.8. Protein production was induced with 0.2 mM 4-(2-Aminoethyl) benzenesulfonyl fluoride hydrochloride (IPTG) overnight at 22°C. Pelleted bacteria were resuspended in 10 mM Tris–HCl pH 8, 200 mM NaCl, 1 mM $CaCl_2$, 1 mM DTT, 50 μg/mL 4-(2-Aminoethyl) benzenesulfonyl fluoride hydrochloride (AEBSF) and 5 U/mL DNase I type II. Bacteria were lysed using a cell

disrupter, and the lysate was cleared from debris at 72,000 g for 60 min in an ultracentrifuge. The supernatant was incubated for 1 h at 4°C with glutathione-Sepharose beads (GE Healthcare) equilibrated in wash buffer (10 mM Tris–HCl pH 8, 200 mM NaCl, 1 mM $CaCl_2$, 1 mM DTT), and applied to a chromatography column. Beads were washed with 100× bead volume of wash buffer before elution of the fusion protein with 30 mM reduced L-glutathione in wash buffer.

For the *in vitro* interaction of Rab7 and RILP, hCTL were washed in PBS, and lysed in 20 mM HEPES pH 7.4, 150 mM NaCl, 5 mM $MgCl_2$, 1% Nonidet P-40, 2 mM GTPγS and ethylenediaminetetraacetic acid (EDTA)-free Protease Inhibitor (Roche Applied Science). Cellular debris was pelleted by centrifugation and the supernantant was pre-cleared by incubation with glutathione Sepharose 4B for 30 min on rotation at 4°C. The cleared lysate was incubated with 5 nmol GST or GST-RILP, respectively, for 1.5 h on rotation at 4°C. Protein material was recovered by incubation with glutathione Sepharose 4B for 2 h on rotation in the cold room. Bound material was washed four times with 20 mM HEPES pH 7.4, 150 mM NaCl, 5 mM $MgCl_2$, 20 μM GTPγS and EDTA-free Protease Inhibitor before elution in sample buffer. Samples were analyzed by SDS–PAGE and immunoblotting using an anti-Rab7 antibody (Sigma).

Acknowledgments

We thank Dr Anna Petrunkina for sorting nucleofected CTL. We thank Dr Angela Wandinger-Ness for providing the anti-Rab7 antibody, Dr Jacques Camonis for anti-RILP, Dr Anna Akhmanova for anti-BICD1 and anti-BICD2 antibodies, and Dr Jacques Neefjes for GFP-RILP and ORP1L-GFP constructs. This work was supported by grants from the Wellcome Trust to G. M. G. Y. H. was funded by Daimler-Benz Foundation, the Cambridge European Trust and Kings College Cambridge.

References

1. Stinchcombe JC, Griffiths GM. Secretory mechanisms in cell-mediated cytotoxicity. Annu Rev Cell Dev Biol. 2007; 23:495–517. [PubMed: 17506701]
2. Bucci C, Thomsen P, Nicoziani P, McCarthy J, van Deurs B. Rab7: a key to lysosome biogenesis. Mol Biol Cell. 2000; 11:467–480. [PubMed: 10679007]
3. Chavrier P, Parton RG, Hauri HP, Simons K, Zerial M. Localization of low molecular weight GTP binding proteins to exocytic and endocytic compartments. Cell. 1990; 62:317–329. [PubMed: 2115402]
4. Lebrand C, Corti M, Goodson H, Cosson P, Cavalli V, Mayran N, Faure J, Gruenberg J. Late endosome motility depends on lipids via the small GTPase Rab7. Embo J. 2002; 21:1289–1300. [PubMed: 11889035]
5. Rink J, Ghigo E, Kalaidzidis Y, Zerial M. Rab conversion as a mechanism of progression from early to late endosomes. Cell. 2005; 122:735–749. [PubMed: 16143105]
6. Cantalupo G, Alifano P, Roberti V, Bruni CB, Bucci C. Rab-interacting lysosomal protein (RILP): the Rab7 effector required for transport to lysosomes. Embo J. 2001; 20:683–693. [PubMed: 11179213]
7. Johansson M, Rocha N, Zwart W, Jordens I, Janssen L, Kuijl C, Olkkonen VM, Neefjes J. Activation of endosomal dynein motors by stepwise assembly of Rab7-RILP-p150Glued, ORP1L, and the receptor betalll spectrin. J Cell Biol. 2007; 176:459–471. [PubMed: 17283181]
8. Jordens I, Fernandez-Borja M, Marsman M, Dusseljee S, Janssen L, Calafat J, Janssen H, Wubbolts R, Neefjes J. The Rab7 effector protein RILP controls lysosomal transport by inducing the recruitment of dynein-dynactin motors. Curr Biol. 2001; 11:1680–1685. [PubMed: 11696325]

9. Johansson M, Lehto M, Tanhuanpaa K, Cover TL, Olkkonen VM. The oxysterol-binding protein homologue ORP1L interacts with Rab7 and alters functional properties of late endocytic compartments. Mol Biol Cell. 2005; 16:5480–5492. [PubMed: 16176980]
10. Hoogenraad CC, Akhmanova A, Howell SA, Dortland BR, De Zeeuw CI, Willemsen R, Visser P, Grosveld F, Galjart N. Mammalian Golgi-associated Bicaudal-D2 functions in the dyneindynactin pathway by interacting with these complexes. Embo J. 2001; 20:4041–4054. [PubMed: 11483508]
11. Combs J, Kim SJ, Tan S, Ligon LA, Holzbaur EL, Kuhn J, Poenie M. Recruitment of dynein to the Jurkat immunological synapse. Proc Natl Acad Sci U S A. 2006; 103:14883–14888. [PubMed: 16990435]
12. Martin-Cofreces NB, Robles-Valero J, Cabrero JR, Mittelbrunn M, Gordon-Alonso M, Sung CH, Alarcon B, Vazquez J, Sanchez-Madrid F. MTOC translocation modulates IS formation and controls sustained T cell signaling. J Cell Biol. 2008; 182:951–962. [PubMed: 18779373]
13. Stinchcombe JC, Majorovits E, Bossi G, Fuller S, Griffiths GM. Centrosome polarization delivers secretory granules to the immunological synapse. Nature. 2006; 443:462–465. [PubMed: 17006514]
14. Spinosa MR, Progida C, De Luca A, Colucci AM, Alifano P, Bucci C. Functional characterization of Rab7 mutant proteins associated with Charcot-Marie-Tooth type 2B disease. J Neurosci. 2008; 28:1640–1648. [PubMed: 18272684]
15. De Luca A, Progida C, Spinosa MR, Alifano P, Bucci C. Characterization of the Rab7K157N mutant protein associated with Charcot-Marie-Tooth type 2B. Biochem Biophys Res Commun. 2008; 372:283–287. [PubMed: 18501189]
16. McCray BA, Skordalakes E, Taylor JP. Disease mutations in Rab7 result in unregulated nucleotide exchange and inappropriate activation. Hum Mol Genet. 2010; 19:1033–1047. [PubMed: 20028791]
17. Marsman M, Jordens I, Rocha N, Kuijl C, Janssen L, Neefjes J. A splice variant of RILP induces lysosomal clustering independent of dynein recruitment. Biochem Biophys Res Commun. 2006; 344:747–756. [PubMed: 16631113]
18. Verhoeven K, De Jonghe P, Coen K, Verpoorten N, Auer-Grumbach M, Kwon JM, FitzPatrick D, Schmedding E, De Vriendt E, Jacobs A, Van Gerwen V, Wagner K, Hartung HP, Timmerman V. Mutations in the small GTP-ase late endosomal protein RAB7 cause Charcot-Marie-Tooth type 2B neuropathy. Am J Hum Genet. 2003; 72:722–727. [PubMed: 12545426]
19. Romero Rosales K, Peralta ER, Guenther GG, Wong SY, Edinger AL. Rab7 activation by growth factor withdrawal contributes to the induction of apoptosis. Mol Biol Cell. 2009; 20:2831–2840. [PubMed: 19386765]
20. Wang T, Hong W. Interorganellar regulation of lysosome positioning by the Golgi apparatus through Rab34 interaction with Rab-interacting lysosomal protein. Mol Biol Cell. 2002; 13:4317–4332. [PubMed: 12475955]
21. Wanschers BF, van de Vorstenbosch R, Schlager MA, Splinter D, Akhmanova A, Hoogenraad CC, Wieringa B, Fransen JA. A role for the Rab6B Bicaudal-D1 interaction in retrograde transport in neuronal cells. Exp Cell Res. 2007; 313:3408–3420. [PubMed: 17707369]
22. Hirokawa N, Noda Y, Tanaka Y, Niwa S. Kinesin superfamily motor proteins and intracellular transport. Nat Rev Mol Cell Biol. 2009; 10:682–696. [PubMed: 19773780]
23. Gross SP. Hither and yon: a review of bi-directional microtubule-based transport. Phys Biol. 2004; 1:R1–R11. [PubMed: 16204815]
24. Cogli L, Piro F, Bucci C. Rab7 and the CMT2B disease. Biochem Soc Trans. 2009; 37:1027–1031. [PubMed: 19754445]
25. Cogli L, Progida C, Lecci R, Bramato R, Kruttgen A, Bucci C. CMT2B-associated Rab7 mutants inhibit neurite outgrowth. Acta Neuropathol. 2010; 120:491–501. [PubMed: 20464402]
26. Yamauchi J, Torii T, Kusakawa S, Sanbe A, Nakamura K, Takashima S, Hamasaki H, Kawaguchi S, Miyamoto Y, Tanoue A. The mood stabilizer valproic acid improves defective neurite formation caused by charcot-marie-tooth disease-associated mutant Rab7 through the JNK signaling pathway. J Neurosci Res. 2010; 88:3189–3197. [PubMed: 20645406]

27. Saxena S, Bucci C, Weis J, Kruttgen A. The small GTPase Rab7 controls the endosomal trafficking and neuritogenic signaling of the nerve growth factor receptor TrkA. J Neurosci. 2005; 25:10930–10940. [PubMed: 16306406]

28. Deinhardt K, Salinas S, Verastegui C, Watson R, Worth D, Hanrahan S, Bucci C, Schiavo G. Rab5 and Rab7 control endocytic sorting along the axonal retrograde transport pathway. Neuron. 2006; 52:293–305. [PubMed: 17046692]

29. Holt O, Kanno E, Bossi G, Booth S, Daniele T, Santoro A, Arico M, Saegusa C, Fukuda M, Griffiths GM. Slp1 and Slp2-a localize to the plasma membrane of CTL and contribute to secretion from the immunological synapse. Traffic. 2008; 9:446–457. [PubMed: 18266782]

30. Jenkins M, Tsun A, Stinchcombe J, Griffiths GM. The strength of the TCR signal controls the polarization of the cytotoxic machinery to the immunological synapse. Immunity. 2009; 31:621–631. [PubMed: 19833087]

31. Zufferey R, Nagy D, Mandel RJ, Naldini L, Trono D. Multiply attenuated lentiviral vector achieves efficient gene delivery in vivo. Nat Biotechnol. 1997; 15:871–875. [PubMed: 9306402]

32. Demaison C, Parsley K, Brouns G, Scherr M, Battmer K, Kinnon C, Grez M, Thrasher AJ. High-level transduction and gene expression in hematopoietic repopulating cells using a human immunodeficiency [correction of imunodeficiency] virus type 1-based lentiviral vector containing an internal spleen focus forming virus promoter. Hum Gene Ther. 2002; 13:803–813. [PubMed: 11975847]

Europe PMC Funders Author Manuscripts

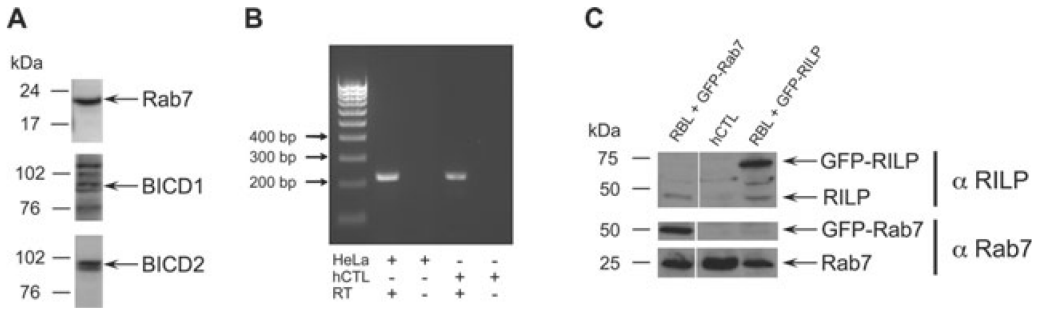

Figure 1. Rab7, Bicaudal and RILP are expressed in CTL

A) Western blots of hCTL lysates probed with antibodies against Rab7 and Bicaudal proteins D1 (BICD1) and D2 (BICD2). B) RT-PCR from HeLa and hCTL mRNA corresponding to a 216-bp fragment of RILP with and without reverse transcriptase (RT). Size markers are shown. C) Western blot of lysates from hCTL (lane 2) or RBL transfected with GFP-Rab7 (lane 1) or GFP-RILP (lane 3) probed with antibodies against RILP or Rab7.

Europe PMC Funders Author Manuscripts

Europe PMC Funders Author Manuscripts

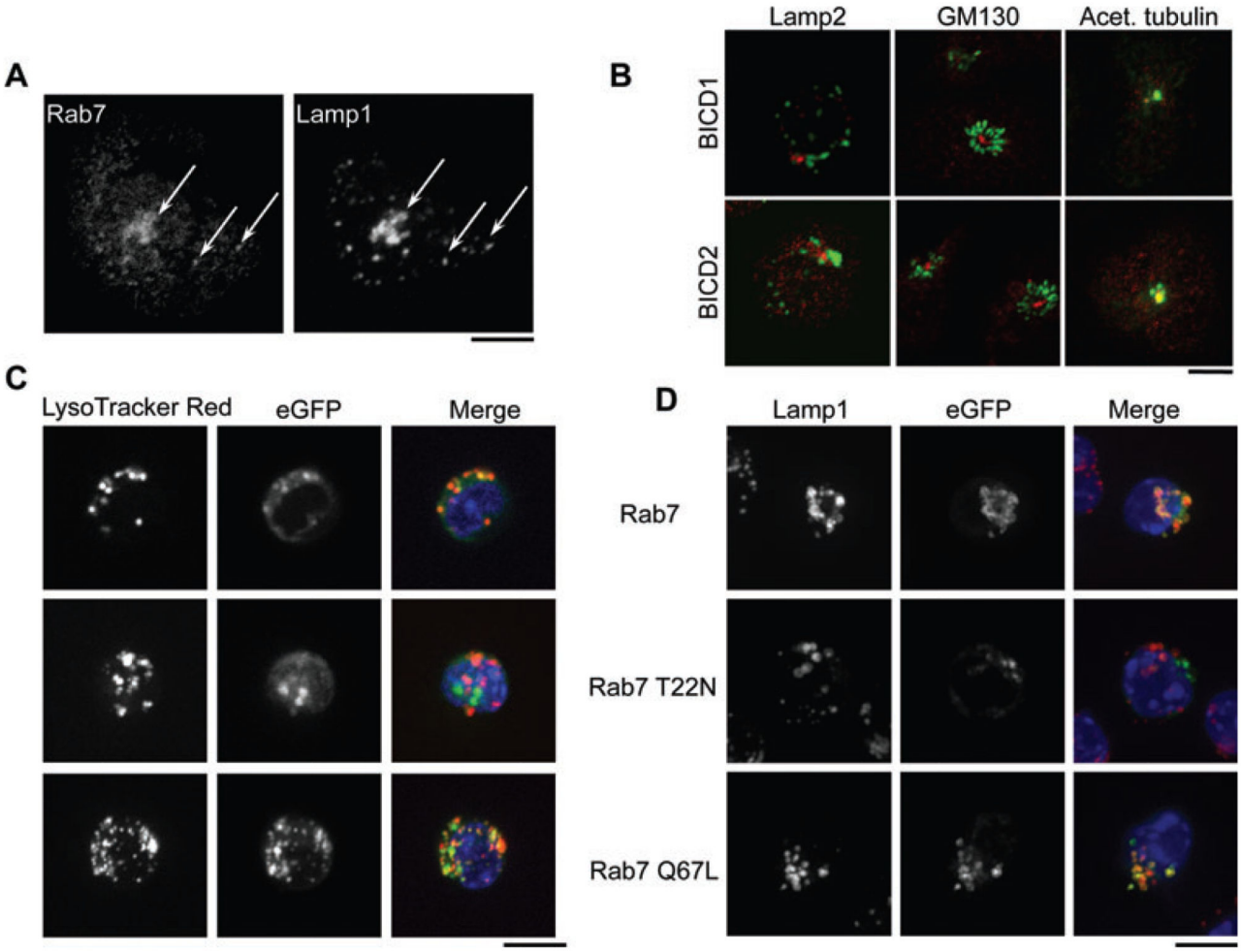

Figure 2. Intracellular localization of Rab7 and BICD1 in CTL

A) hCTL labeled with antibodies against Rab7 and Lamp1. Arrows indicate colocalization. B) hCTL labeled with antibodies against BICD1 or BICD2 (red) and Lamp2, GM130 or acetylated tubulin (green), as indicated. C) Representative images of live OT-1 mCTL nucleofected with GFP-tagged human Rab7 constructs (as indicated) imaged with Lysotracker (lysosomes, red) and Hoechst (nuclei, blue) or (D) fixed after 24 h and stained with anti-Lamp1. Scale bars: (A) 5 μm; (B) 3 μm; (C,D) 10 μm.

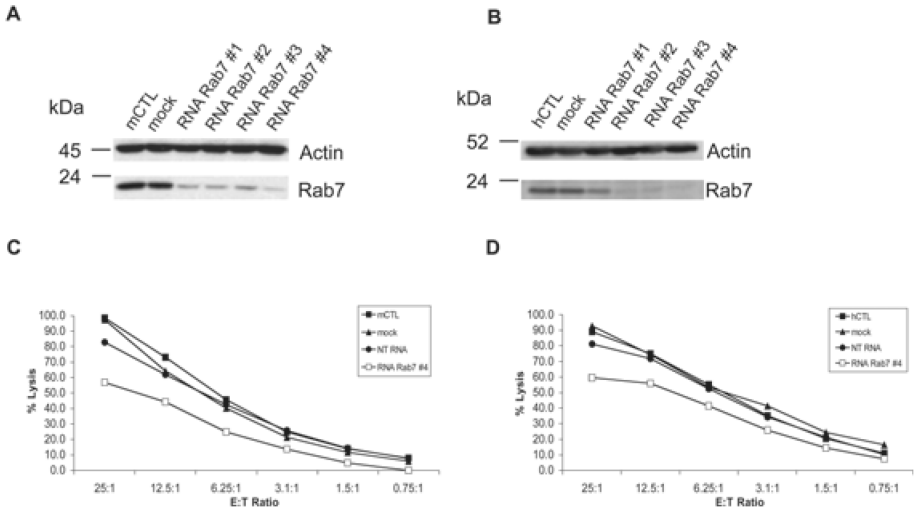

Figure 3. Rab7 silencing reduces CTL cytotoxicity

mCTL (A and C) or hCTL (B and D) were nucleofected with 3 μg of siRNAs 1–4 against Rab7 (RNA Rab7), NT RNA or no siRNA (Mock) as indicated. A,B) Western blots of cell lysates probed with antibodies against Rab7 and actin. C and D) Killing assays showing percentage target cell lysis at different ratios of effector CTL (E) to target P815 (T). Graphs show a representative result from three independent experiments, each performed in triplicate. Standard deviations for triplicates were less than 4%.

Europe PMC Funders Author Manuscripts

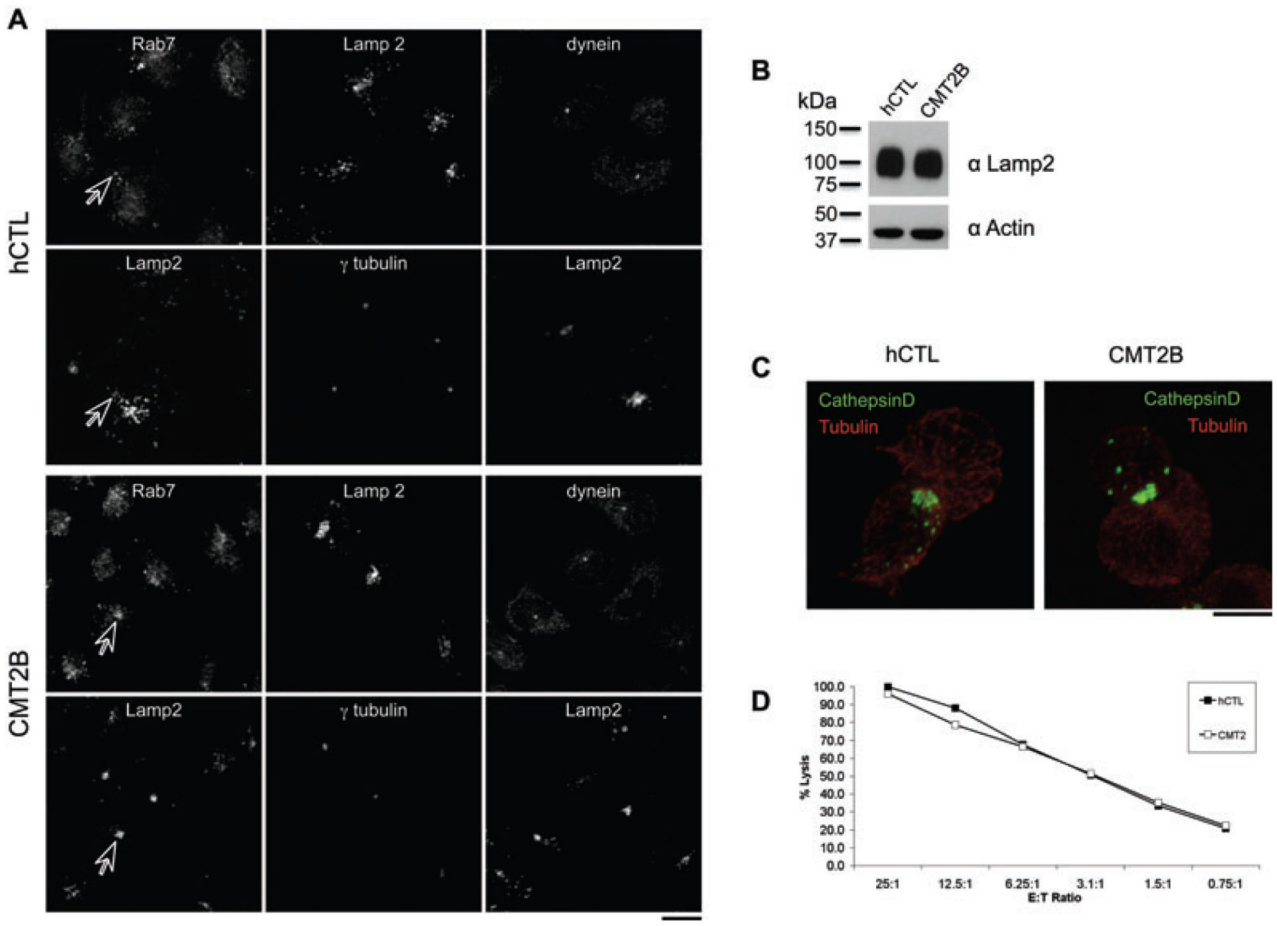

Figure 4. Rab7 V162M mutation neither impairs nor enhances CTL killing

A) CD8 positive bulk of cells generated from healthy donor (hCTL) and patients affected by the CMT2B with the V162M mutation in Rab7, stained for Rab7, Lamp2 and dynein. Arrows indicate organelles labeled by Rab7 and Lamp2. B) Western blot of cell lysates from hCTL from healthy donors or CMT2B cell lines probed with anti-Lamp2 (H4B4) and actin. Molecular weight markers are shown. C) CTL-target conjugates from hCTL and CMT2B labeled with antibodies to cathepsin D (green) and tubulin (red). D) Killing assay showing the percent lysis of targets at different ratios of effector CTL (E) to target P815 (T). Graph shown is representative of two independent experiments, each performed in triplicate. Standard deviations from triplicates were less than 2%. Scale bars: 5 μm.

Europe PMC Funders Author Manuscripts

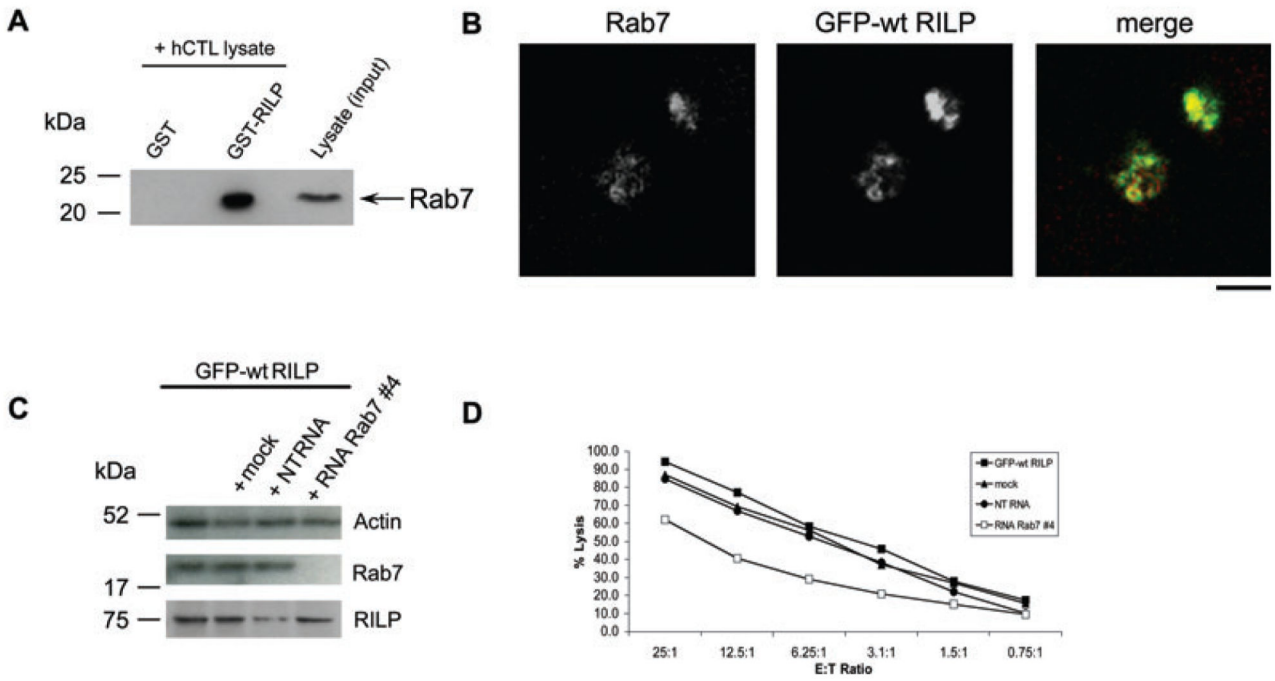

Figure 5. Rab7 interacts with RILP in hCTL

A) GST and GST-tagged RILP were incubated with hCTL cell lysate pretreated with 2 mM GTPγS, subjected to WB and probed with an anti-Rab7 antibody (Sigma) to detect the endogenous protein. B) hCTL transduced with GFP-RILP stained with anti-Rab7. C) Western blot of lysates from hCTL transduced with GFP-wt RILP (GFP-wt RILP) mock-treated (mock) or nucleofected with 3 μg of non-targeting (NT RNA) or RNA duplexes against human Rab7 (RNA Rab7 #4) as indicated, probed with anti-Rab7 and anti-RILP antibodies, using actin as a loading control. D) Killing assay showing the percentage lysis of targets at different ratios of effector CTL (E) to target P815 (T). Graph shown is representative of two independent experiments, each performed in triplicate. Standard deviations of triplicates were less than 5%. Scale bar: 3 μm.

Europe PMC Funders Author Manuscripts

Europe PMC Funders Author Manuscripts

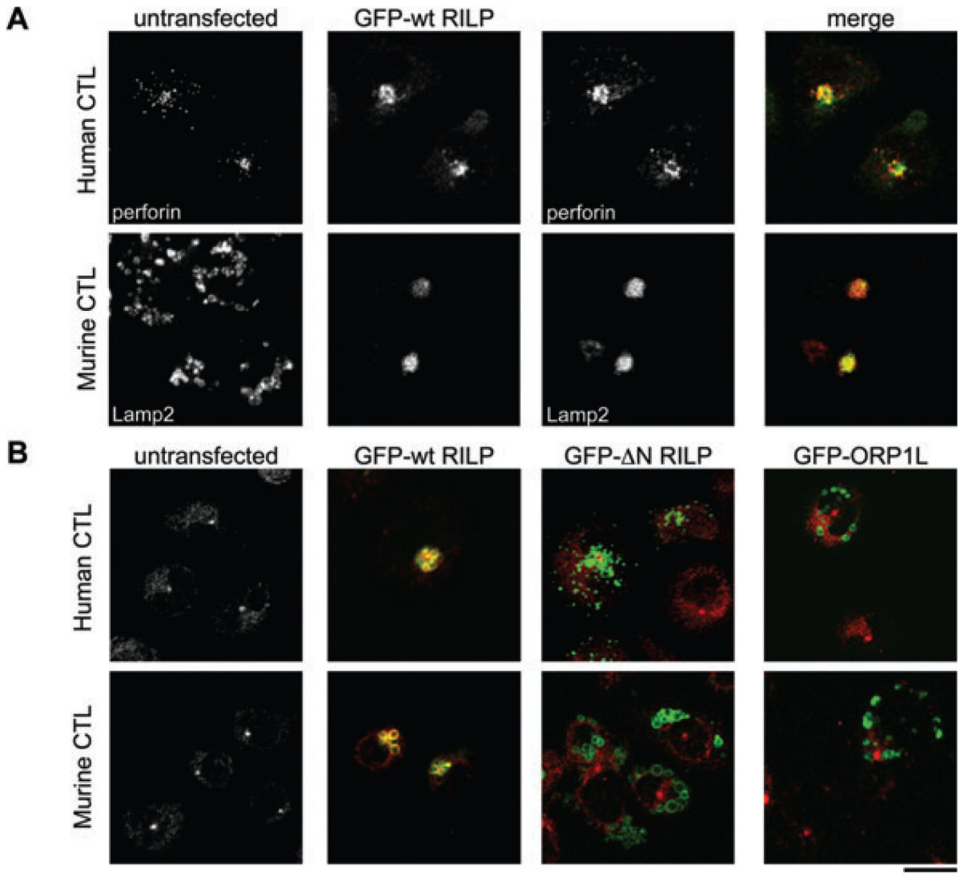

Figure 6. RILP over-expression recruits dynein to the lysosomes of CTL

A) hCTL or mCTL untransfected or transiently transfected with GFP-wt RILP and labeled for perforin (hCTL, red) or LAMP2 (mCTL, red). B) hCTL or mCTL untransfected or transiently transfected with GFP-wt RILP, GFP-N RILP or GFP-ORP1L and labeled with anti-dynein (red). Scale bar: 10 μm.